Photoacoustic mammography: initial clinical results

Toshiyuki Kitai[1], Masae Torii[1], Tomoharu Sugie[1], Shotaro Kanao[2], Yoshiki Mikami[3], Tsuyoshi Shiina[4], Masakazu Toi[1]

1. Department of Breast Surgery, Graduate School of Medicine, Kyoto University
2. Department of Diagnostic Imaging and Nuclear Medicine, Graduate School of Medicine, Kyoto University
3. Department of Diagnostic Pathology, Graduate School of Medicine, Kyoto University
4. Department of Human Health Science, Graduate School of Medicine, Kyoto University

Corresponding author: Toshiyuki Kitai, MD, PhD

Department of Breast Surgery, Graduate School of Medicine, Kyoto University

54 Kawaracho Shogoin Sakyoku, Kyoto 6068507, Japan

Tel.: +81757513660, fax: +81757513161

E-mail: kitait@kuhp.kyoto-u.ac.jp

Abstract

Purpose: Photoacoustic tomography can make an image of hemoglobin distribution and oxygenation state inside tissue with high spatial resolution. The purpose of this study is to investigate its clinical usefulness for the diagnosis of breast cancer and the evaluation of therapeutic response in relation to other diagnostic modalities.

Materials and methods: Using a prototype machine for photoacoustic mammography (PAM), 27 breast tumor lesions, including 21 invasive breast cancer (IBC), five ductal carcinoma in situ (DCIS) and one phyllodes tumor, were measured. Nine out of twenty one IBC patients had received primary systemic therapy (PST).

Results: Eight out of twelve IBC without PST were visible. Notably, detection was possible in all five cases with DCIS, whereas it was not in one case with phyllodes tumor. Seven out of nine IBC with PST were assigned as visible in spite of decreased size of tumor after PST. The mean value of hemoglobin saturation in the visible lesions was 78.6 %, and hemoglobin concentration was 207 μM. The tumor images of PAM were comparable with those of MRI.

Conclusions: It was suggested that PAM can provide images on tumor vascularity and oxygenation which may be useful for the diagnosis and characterization of breast cancer.

Key words: photoacoustic mammography, optical imaging, near-infrared, breast cancer, tumor vascularity, oxygenation

Introduction

Breast cancer is one of the most common malignant diseases in women. Early detection and diagnosis are essential to decrease the mortality. In addition, as the number of cases of primary systemic therapy (PST) increases, efforts have been made to develop a sensitive method for monitoring the treatment effect [1, 2]. Conventional diagnostic modalities, including X-ray mammography (MMG), ultrasonography (US), and magnetic resonance imaging (MRI), are useful for these purposes, but each has some drawbacks. Mammography is associated with ionizing radiation and has diagnostic weakness for dense breast. The results of ultrasound greatly depend on the instrumental performance and examiner's skill. MRI requires the use of contrast medium, which is not suitable for mass screening and repeated examination.

Optical detection of breast cancer using near-infrared (NIR) light has drawn much attention because it can measure hemoglobin distribution and oxygenation state inside the tissue noninvasively [4, 5]. Angiogenesis is essential for breast cancer growth and also correlated with the malignant potential of precursor lesion [6-9]. It is known that microvessel density in the cancer tissue significantly decreases in the responders for PST from the early period [10]. Therefore, optical imaging has great potential as the basis of novel diagnostic modalities for breast cancer. Several studies have reported promising results for diffuse optical tomography (DOT) used for differential diagnosis and therapeutic monitoring of breast cancer [11-17]. However, at

present, its clinical usefulness seems to be limited due to poor spatial resolution. Photoacoustic tomography is another modality of optical imaging based on photoacoustic technology, which can make an image of hemoglobin distribution and oxygenation state inside tissue with higher spatial resolution than DOT [18- 20]. There are a few preliminary reports on such approaches for breast cancer [21-23].

In this paper, we report early results for the clinical application of PAM and investigate its usefulness for the diagnosis of breast cancer and the evaluation of therapeutic response in relation to other diagnostic modalities.

Materials and methods

Instruments

A prototype machine of a dual illuminated mode photoacoustic tomography system (Canon Inc., Tokyo, Japan) was used [24, 25]. Figure 1 shows a photograph of the machine and a schematic description of the measurement. The patient-instrument interface was a sliding bed with a hole of 17 cm by 18 cm, which was mounted on the frame housing laser-emitting and ultrasound detection units. The patient lay in a prone position on the bed with her breast placed in the hole. The breast was mildly compressed in a cranio-caudal direction between holding plates. Acoustic coupling gel was used between the breast and the holding plate that carried the scanning system. Pulsed laser beams were irradiated to the breast from both sides and the photoacoustic signals were detected on the caudal side by

an array transducer. The lasers were mounted at the bottom of the bed and coupled to the scanning system. A Ti:Sa laser optically pumped with a Q-switched Nd:YAG laser, having a tunable wavelength of 700 to 900 nm. The measurable area was 30 mm by 46 mm for one scan, which took 45 seconds. In the first 16 cases, the scan was performed at three adjacent areas where the lesion was considered to be located in the diseased breast and one area in the intact breast. In the last 15 cases, the scanning system was automatically moved in an area of 120 mm by 46 mm. Specific parameters of the PAM are as follows:

Laser	Wavelength	1064, 825, 797, 756 nm
	Pulse width	7 ns
	Repetition rate	10 Hz
Detector	Matrix shape	Rectangular
	Number of elements	15 by 23
	Element size	2 by 2 mm
	Central frequency	1 MHz

Photoacoustic image reconstruction was carried out using a modified universal backprojection algorithm. Assuming that the breast consisted of homogeneous tissue with known μa and μs', the μa values of the absorbers were calculated from the initial pressure rise after the laser pulse using the equation as shown below [4]. Light fluence distribution inside the breast was estimated using the published data of absorption and scattering coefficients (μa and μs') of the breast corresponding to the patients' age [26].

$$p_0 = \Gamma\eta_{th}\mu_a F$$

p_0 : initial pressure after the laser pulse

Γ : Grueneisen parameter. At body temperature, $\Gamma = 0.20$

η_{th} : percentage that is converted into heat

μ_a : absorption coefficient

F : light fluence

Thus, the distribution of μa in the breast was calculated from the initial pressure distribution at each wavelength. Oxygen saturation of hemoglobin (SO_2) and total hemoglobin concentration (THC) of the lesions were calculated using μa values at 797 nm and 756 nm. Extinction coefficients of oxyhemoglobin and deoxyhemoglobin were used as 0.231 and 0.259 at 797 nm, and 0.163 and 0.511 at 756 nm, respectively.

Patients

Thirty-one patients, who were histologically diagnosed with breast cancer or phyllodes tumor, were recruited in this study at Kyoto University Hospital from August 2010 to July 2011. Twenty seven breast lesions of twenty-six cases were subjected to analysis. The other five cases were excluded from analysis because the tumor was outside of the measurable area of PAM for the reason that the breast was too small or the tumor was located very near the chest wall. MMG, US, and MRI were undertaken as routine preoperative workup. All patients underwent breast surgeries

following PAM measurements within one month, and no anti-cancer treatment was given during the interval. The excised specimens were pathologically examined. For assignment of the pathological effect of PST, Histopathological Criteria for Assessment of Therapeutic Response of Japanese Breast Cancer Society were used [24], which assigned the pathological effect as grade 0 (no response) to grade 3 (complete response). Visibility assignment of PAM image was made by one of the authors who is a radiologist specialized in the diagnosis of breast cancer. Our procedures were as follows; signals which were supposed to come from vascular rich lesions or vessels were extracted from PAM images without considering clinical data including other imaging modalities. The selection criteria were the intensity and the morphology of the signal. Linear, winding or branched shaped signals were attributed to the vessels. Grouped or locally scattered signals were attributed to the vascular rich lesion. Usually, several signals or groups were extracted from one breast measurement. Each PAM signal, then, was correlated with that of MRI by comparing the locations. The assignment of the location was adjusted by the shape of subcutaneous veins which were demonstrated by both of PAM and MRI. When any signal was found to be located at the site of the tumor of known, the radiologist judged whether the signal was associated with the tumor considering the intensity, the shape and the distribution.

The study protocol was approved by the Medical Ethical Committee of Kyoto University.

Results

The average age was 58.0 years (36 ~ 83 years), and the tumor size measured by MRI was 20.1 mm (11 ~ 70 mm). Preoperative diagnosis was invasive breast cancer (IBC) in twenty one breasts, including twenty invasive ductal carcinomas (IDC), one invasive lobular carcinoma (ILC), ductal carcinoma in situ (DCIS) in five cases, and phyllodes tumor in one case. Biological subtype of IBC was ER+/HER2- in eighteen lesions, ER-/HER2+ in two, and ER-/HER2- in one. PST was given in 9 out of 21 IBC patients.

The tumor was assigned as visible by PAM in 20 out of 27 breasts (74 %), as shown in Table 1. Table 2 shows the results of IBC cases without PST. Eight out of twelve IBC were visible. Table 3 shows the results with PST. Five out of nine cases showed clinical partial response and pathological therapeutic effect better than grade 2 (marked response). Seven cases were assigned as visible in spite of decreased size of tumor after PST. Table 4 shows the results of DCIS and phyllodes tumor. Notably, detection was possible in all five cases with DCIS. On the other hand, it was not possible with phyllodes tumor. A mean value of SO_2 in the visible lesions was 78.6 % (53.7 ~ 100%), and THC was 207 µM (87 ~ 309 µM).

Two particular cases of IBC with or without PST are now presented in detail.

1) IBC without PST

The patient was a 75-year-old woman with left breast cancer. MRI showed a tumor with ring enhancement with a diameter of 22 mm.

Pathological diagnosis was IDC (ER+/HER2+). At PAM measurement, the breast was compressed to a thickness of 58 mm. Figure 2 shows subcutaneous blood vessels by PAM. The value of SO_2 ranged from 92.1% to 98.6%. Figure 3 shows a maximum intensity projection (MIP) image of PAM at a depth between 7.75 and 11.5 mm, indicating clustered signals aligned in a ring shape and a linear-shaped signal. These signals were comparable with the MRI findings and considered to represent the tumor and the feeding vessel, respectively. Mean values of SO_2 and THC in the areas with these signals were 87.1% and 112 μM, respectively.

2) IBC after PST

The patient was a 41-year-old woman with right breast cancer. The tumor was reduced in size from 34 mm to 22 mm in diameter after six-month treatment with endocrine therapy. PAM image at a depth of 28.25 mm showed signals comparable with those of MRI image (Figure 4). Pathological diagnosis was IDC (ER+/HER2-) and the therapeutic effect was assigned as grade 1b (moderate response). Mean values of SO_2 and THC of the two assigned lesions were 74.5 % and 385 μM in A area, and 53.8 % and 307 μM in B area, respectively.

Discussion

Photoacoustic tomography refers to imaging that is based on the photoacoustic effect [4, 18-20]. When light is emitted into the tissue, some of

the light is absorbed by the object and partially converted into heat. The heat is then further converted to a pressure rise via thermoelastic expansion. The pressure rise is propagated as an ultrasonic wave, which is detected by ultrasonic transducers and is used by a computer to form an image. The purpose of using photoacoustic tomography is to combine the contrast of optical absorption with the spatial resolution of ultrasound for deep imaging of living tissue. Since optical absorption provides biological information about tissue vascularization and oxygenation state, functional imaging regarding tissue oxygenation can be obtained. Previous reports using animal models showed successful results on imaging of lympho-vascular structure inside tissue [20, 28, 29]. This technology has already been applied to breast cancer patients [21, 23], but the clinical evaluation was limited.

We compared PAM images with MRI, since MRI is currently the most accurate imaging method for determining the extent of disease in the breast [30, 31]. As shown in Fig. 3 and 4, the tumor image of PAM was comparable with that of MRI demonstrating rim enhancement. These findings could be attributable to the distribution of higher vascular densities in the peripheral area of cancer. However, the tumor image of PAM was not mass-forming as shown by MRI. Discrepancy in the image presentation probably arises from the difference in distribution of contrast materials. Photoacoustic image represents the distribution of hemoglobin inside the vessels, whereas MRI image presents not only the tumor vessels but also the surrounding stroma where the contrast media is shed out from the vessels. In a preliminary study using animals and excised breast cancer specimens, the intensity of

PAM signal was correlated with the microvessel density in the tumor tissue (data not shown).

In this study, 20 out of 27 breast cancer lesions were assigned as visible in PAM images. The detection rate seems acceptable, considering the variety of cases in this series. Previous clinical studies reported PAM images of breast cancer corresponding to the findings of MMG or US (21, 23) and detection rate similar to ours (23), but the patient population was rather homogeneous. This study evaluated PAM images in cases of DCIS and IDC with PST as well. Reasons of failure in unsuccessful cases of IBC without PST were mostly the small size of the breast, the breast surface deformity and the poor vascularity of the tumor.

Five cases of DCIS with diameters of 63 mm and 11 mm were visible by PAM but phyllodes tumor with a diameter of 35 mm was not. These results suggest that PAM may be useful to differentiate malignant lesions from benign ones and also to detect breast cancer at an early stage. It was reported that microvascular density increased at the stage of non-invasive carcinoma [7, 9]. Previous studies of DOT also showed that tissue hemoglobin concentration was a good parameter to differentiate between malignant and benign lesions [15, 17]. High spatial resolution of PAM would be beneficial for the detection of small DCIS lesions. Further study is necessary to confirm these hypotheses.

Seven out of nine cases after PST could be detected by PAM in spite of decreased diameter and cellularity of the tumor. As the number of cases of PST increases, sensitive measures monitoring therapeutic effect are

required [32-35]. As well as radiological imaging modalities and biological markers of biopsy specimens, promising results have been reported for optical imaging using DOT. It has been reported that hemoglobin concentration decreased during PST before morphological changes appeared and that oxygen saturation transiently increased shortly after the start of PST [12, 16]. Since repeated examinations along the treatment course are necessary, the non-invasiveness of optical imaging is beneficial. In addition, PAM has the possibility to monitor not only changes in hemoglobin in the whole tumor but also changes at a higher resolution within the tumor. Quantitative evaluation of tumor images by PAM must be established for the purpose of monitoring the effect of PST.

This study used multiple wavelengths to measure PAM signals to estimate the tumor SO_2 and THC, which was the first attempt of its kind in clinical studies. It has been reported that malignant tumor has a higher THC and lower SO_2 than background breast tissue. According to a review paper on DOT [17], tumor showed THC of 65 ± 34 μM, which were 2.0~4.5-fold higher than the background THC. The tumor SO_2 was 66 ± 24 %, which was 0.8~0.82 fold that of the background SO_2. The values of THC and SO_2 of 207 μM and 78.6 %, respectively, in breast cancer calculated in this study were higher than the reported data of DOT. These discrepancies are partly due to the difference in spatial resolution between the two imaging modalities. Contrast of the tumor arises from the difference of hemoglobin concentration between tumor and normal breast tissues in both PAM and DOT. PAM may select a more confined area where the tissue is more vascular-rich and

oxygenated than the area defined by DOT. However, there are several problems in quantitative evaluation of SO2 and THC by PAM; 1) Light distribution in the breast tissue at each wavelength should be known a priori. We used μa and μs' values reported in the past literature to calculate the light distribution, but some deviation from the actual distribution might exist in each case. 2) The direction of the vessels and the shape of absorbers should affect the intensity of PAM signals. 3) Noise occurring at the margin of the breast and the boundaries of the compression plates prevents the quantitative measurement of initial pressure of thermo-elastic wave. Noise reduction is essential to quantitative evaluation of optical parameters. Further study is necessary to quantify these optical parameters for clinical use.

Breast compression is an inevitable problem with the present method. We compressed the breast for two reasons: one is to make contact with the plate carrying the ultrasound detectors and the other is to increase the light fluence rate inside the breast by decreasing the breast thickness. However, compression at high pressure may disturb the tissue circulation [36]. Care was taken to apply minimal pressure so as not to change the tissue circulation and oxygenation. In fact, clear demonstration of subcutaneous vasculature and reasonable SO_2 values suggested that the tissue circulation was fairly well maintained.

PAM could provide images of tumor vasculature and oxygenation, which cannot be obtained by MMG or US. However, imaging depth and resolution still require improvement. At present, PAM has an advantage in

terms of functional features rather than morphology. The combination of PAM with US, as demonstrated in animal models [24, 25], would be useful to achieve more comprehensive imaging of breast cancer, where the biological and anatomical aspects can be assessed simultaneously. It was suggested that PAM can be useful for the diagnosis and characterization of breast cancer and its further clinical exploration is promising.

References

1) Smith PA, D'Orsi C, Newell MS. Screening for breast cancer. In: Harris JR, Lippman ME, Morrow M, Osborne CK, editors. Disease of the Breast. 4th ed. Philadelphia: Lippincott – Williams & Wilkins; 2010. P. 87-115.

2) Gounaris I, Provenzano E, Vallier AL, Hiller L, Iddawela M, Hilborne S, et al. Accuracy of unidimensional and volumetric ultrasound measurements in predicting good pathological response to neoadjuvant chemotherapy in breast cancer patients. Breast Cancer Res Treat. 2011;127:459-69

3) Chen JH, Feig BA, Hsiang DJ, Butler JA, Mehta RS, Bahri S, et al. Impact of MRI-evaluated neoadjuvant chemotherapy response on change of surgical recommendation in breast cancer. Ann Surg. 2009; 249:448-54.

4) Biomedical optics principles and imaging, Wang LV, Wu HI. Hoboken: Wiley-Interscience; 2007.

5) Frangioni JV. New technologies for human cancer imaging. J Clin Oncol. 2008;26:4012-21.

6) Brem SS, Jensen HM, Guillino PM. Angiogenesis as a marker of preneoplastic lesions of the human breast. Cancer. 1978;41:239-44.

7) Viacava P, Naccarato AG, Bocci G, Fanelli G, Aretini P, Lonobile A, et al. Angiogenesis and VEGF expression in pre-invasive lesions of the human breast. J Pathol. 2004;204:140-6.

8) Uzzan B, Nicolas P, Cucherat M, Perret GY. Microvessel density as a prognostic factor in women with breast cancer: a systematic review of the literature and meta-analysis. Cancer Res. 2004;64:2941-55.

9) Guidi AJ, Fischer L, Harris JR, Schnitt SJ. Microvessel density and distribution in ductal carcinoma in situ of the breast. J Natl Cancer Inst. 1994;86:614-9.

10) Makris A, Powles TJ, Kakolyris S, Dowsett M, Ashley SE, Harris AL. Reduction in angiogenesis after neoadjuvant chemoendocrine therapy in patients with operable breast carcinoma. Cancer. 1999;85:1996-2000.

11) Jiang S, Pogue BW, Carpenter CN, Poplack SP, Wells WA, Kogel CA, et al. Evaluation of breast tumor response to neoadjuvant chemotherapy with tomographic diffuse optical spectroscopy: case studies of tumor region-of-interest changes. Radiology. 2009;252:551-60.

12) Soliman H, Gunasekara A, Rycroft M, Zubovits J, Dent R, Spayne J, et al. Functional imaging using diffuse optical spectroscopy of neoadjuvant chemotherapy response in woman with locally advanced breast cancer. Clin Cancer Res. 2010;16:2605-14.

13) Zhu Q, Hegde PU, Ricci A, Kane M, Cronin EB, Ardeshirpour Y, et al. Early-stage invasive breast cancers: Potential role of optical tomography with US localization in assisting diagnosis. Radiology. 2010;256:367-78.

14) Tromberg BJ, Pogue BW, Paulsen KD, Yodh AG, Boas DA, Cerussi AE. Assessing the future of diffuse optical imaging technique for breast cancer management. Med Phys. 2008;35:2443-51.

15) Choe R, Konecky SD, Corlu A, Lee K, Durduran T, Busch DR, et al. Differentiation of benign and malignant breat tumors by in vivo three-dimensional parallel-plate diffuse optical tomography. J Biomed Opt. 2009;14:024020.

16) Roblyer DM, Ueda S, Cerussi AE, Tanamai W, Durkin A, Mehta RS, et al. Oxyhemoglobin flare after the first day of neoadjuvant breast cancer chemotherapy predicts overall response. Cancer Res. 2010;70:363s.

17) Leff DR, Warren OJ, Enfield LC, Hebden J, Yang GZ, Darzi A. Diffuse optical imaging of the healthy and diseased breast: A systematic review. Breast Cancer Res Treat. 2008;108:9-22.

18) Emelianov S, Li P-C, O'Donnell M. Photoacoustics for molocular imaging and therapy. Phys Today. 2009;62:34-9.

19) Laufer J, Delpy D, Elwell C, Beard P. Quantitative spatially resolved measurement of tumor chromophore concentrations using photoacoustic spectroscopy: application to the measurement of blood oxygenation and hemoglobin concentration. Phys Med Biol. 2007;52:141-68.

20) Zhang EZ, Laufer JG, Pedley RB, Beard PC. In vivo high-resolution 3D photoacoustic imaging of superficial vascular anatomy. Phys Med Biol. 2009;54:1035-46..

21) Manohar S, Vaartjes SE, Hespen JCG, Klasse JM, Engh FM, Steenbergen W, et al. Initial results of in vivo non-invasive cancer imaging in the human breast using near-infrared photoacoustics. Opt Express. 2007;15:12277-85.

22) Kruger RA, Lam RB, Reinecke DR, Del Rio SP, Doyle RP. Photoacoustic

angiography of the breast. Med Phys. 2010;37:6096-100.

23) Ermilov SA, Khamapirad T, Conjusteau A, Leonard MH, Lacewell R, Mehta K, et al. Laser optoacoustic imaging system for detection of breast cancer. J Biomed Opt. 2009;14:024007.

24) Fukutani K, Someda Y, Taku M, Asao Y, Kobayashi S, Yagi T, et al. Characterization of photoacoustic tomography system with dual illumination. Proc SPIEE 2011.

25) Tanji K, Watanabe K, Fukutani K, Asao Y, Yagi T. Yamakawa M, et al. Advanced model-based reconstruction algorithm for practical three-dimensional photo acoustic imaging. Proc SPIEE 2011.

26) Suzuki K, Yamashita Y, Ohta K, Kaneko M, Yoshida M, Chance B. Quantitative measurement of optical parameters in normal breasts using time-resolved spectroscopy in vivo results of 30 Japanese women. J Biomed Opt. 1996;1:330-4.

27) Kurosumi M, Akashi-Tanaka S, Akiyama F, Komoike Y, Mukai H, Nakamura S, et al. Histopathological criteria for assessment of therapeutic response in breast cancer (2007 version). Breast Cancer. 2008;15:5-7.

28) Kim C, Song KH, Gao F, Wang LV. Sentinel lymph nodes and lymphatic vessels: noninvasive dual-modality in vivo mapping by using indocyanine green in rats – volumetric spectroscopic photoacoustic imaging and planer fluorescence imaging. Radiology. 2010;255:442-50.

29) Erpelding TN, Kim C, Pramanik M, Jankovic L, Maslov K, Guo Z, et al. Sentinel lymph nodes in the rat: Noninvasive photoacoustic and US

imaging with a clinical US system. Radiology. 2010;256:102-10.

30) Orel SG, Schnall MD. MR imaging of the breast for the detection, diagnosis, and staging of breast cancer. Radiology. 2001;220:13-30.

31) Tse GM, Chaiwun B, Won KT, Yeung DK, Pang AL, Tang AP, et al. Magnetic resonance imaging of breast lesions – a pathological correlation. Breast Cancer Res Treat. 2007;103:1-10.

32) Chuah BY, Putti T, Salto-Tellez M, Charlton A, Iau P, Buhari SA, et al. Serial changes in the expression of breast cancer-related proteins in response to neoadjuvant chemotherapy. Ann Oncol. 2011;22:1748-54.

33) Smith IE, Dowsett M, Ebbs SR, Dixon JM, Skene A, Blohmer YU, et al. Neoadjuvant treatment of postmenopausal breast cancer with anastrozole, tamoxifen, or both in combination : The immediate preoperative anastrozole, tamoxifen, or combined with tamoxifen (IMPACT) multicenter double-blind randomized trial. J Clin Oncol. 2005;23:5108-16.

34) Jacobs MA, Ouwerkerk R, Wolff AC, Gabrielson E, Warzecha H, Jeter S, et al. Monitoring of neoadjuvant chemotherapy using mutiparametric, (23)Na sodium MR, and multimodality (PET/CT/MRI) imaging in locally advance breast cancer. Breast Cancer Res Treat. 2011;128:119-26.

35) Loo CE, Straver ME, Rodenhuis S, Muller SH, Wesseling J, Vrancken Peeters MJ, et al. Magnetic resonance imaging response monitoring of breast cancer during neoadjuvant chemotherapy: relevance of breast cancer subtype. J Clin Oncol. 2011;29:660-6.

36) Wang B, Povoski SP, Cao X, Sun D, Xu RX. Dynamic schema for near

infrared detection of pressure-induced changes in solid tumors. Appl Opt. 2008;47:3053-63.

Figure Legends

Fig. 1

a) A photograph of the prototype machine: The patient-instrument interface was a sliding bed with a hole of 17 cm by 18 cm. The lasers were mounted at the bottom of the bed and coupled to the ultrasound scanning system.

b) A schematic description of PAM measurement: Near-infrared laser pulse was irradiated to the breast and thermoelastic waves produced by absorbers in the breast were detected by ultrasound detectors.

Fig. 2

Subcutaneous blood vessels were clearly shown (depth: 1.5~2.25 mm). The SO_2 values ranged from 92.1 % to 98.6 %

Fig. 3

IBC without PST

Upper panel: PAM image showed clustered signals aligned in a ring (dotted circle) and a linear signal (arrow) (depth: 7.75~11.5 mm, breast thickness: 58 mm). These signals were considered to represent the tumor and the feeding vessel, respectively. Mean values of SO_2 and THC of the tumor were 87.1% and 112 μM, respectively.

Lower panel: MRI showed a tumor with ring enhancement. The dotted square corresponds to the area of the PAM image.

Fig. 4

IBC after PST

Upper panel: PAM image showed clustered signals (squared areas A and B). (depth: 28.25 mm, breast thickness: 68 mm). Area A and B were assigned as peripheral part and central part of the tumor, respectively.   Mean values of SO_2 and THC of the assigned lesions were (A) 74.5 % and 385 μM, and (B) 53.8 % and 307 μM, respectively.

Lower panel: MRI showed an enhanced tumor of 22 mm in size. The dotted square corresponds to the area of the PAM image.
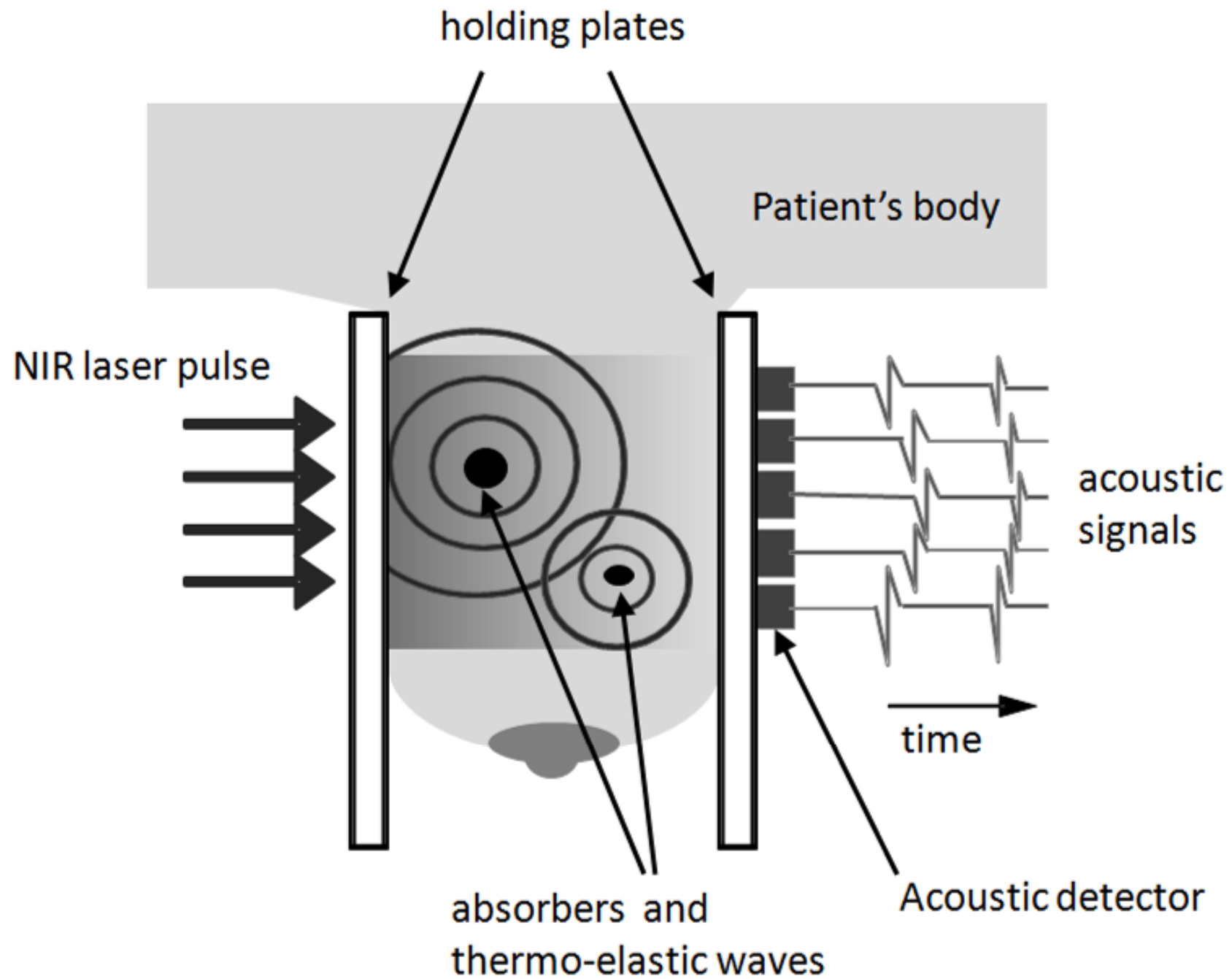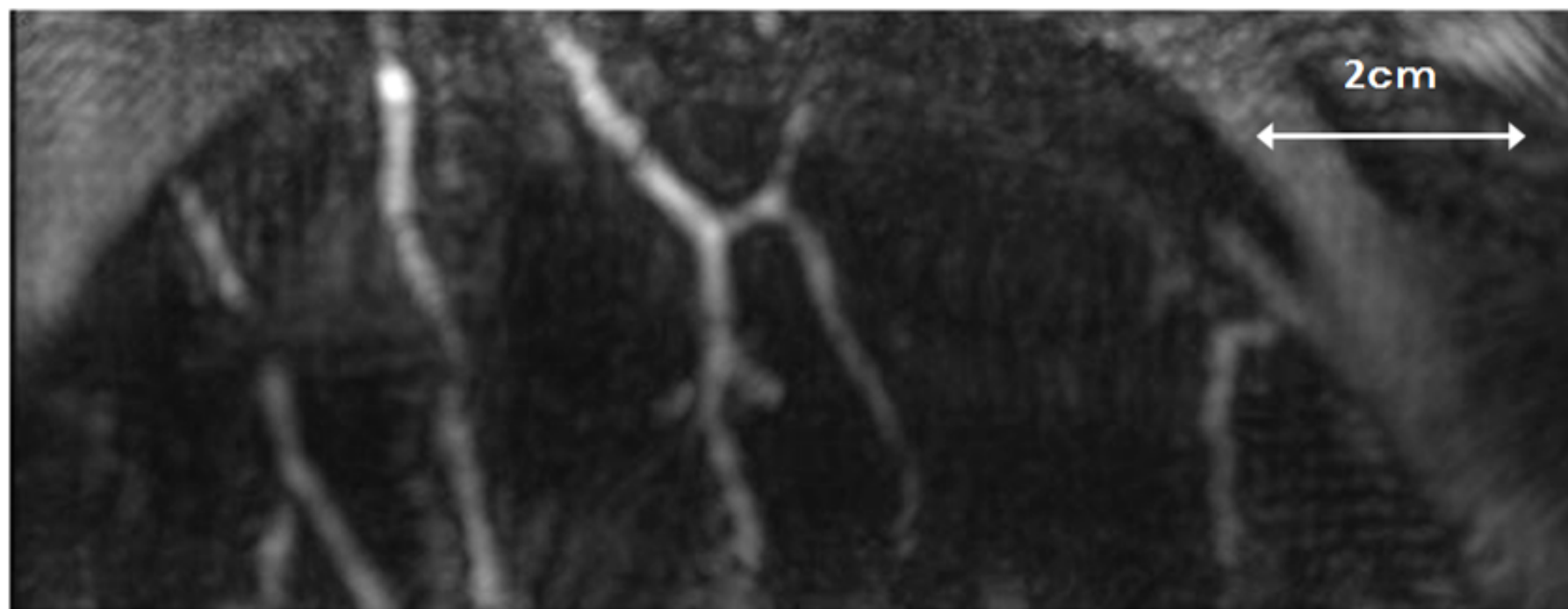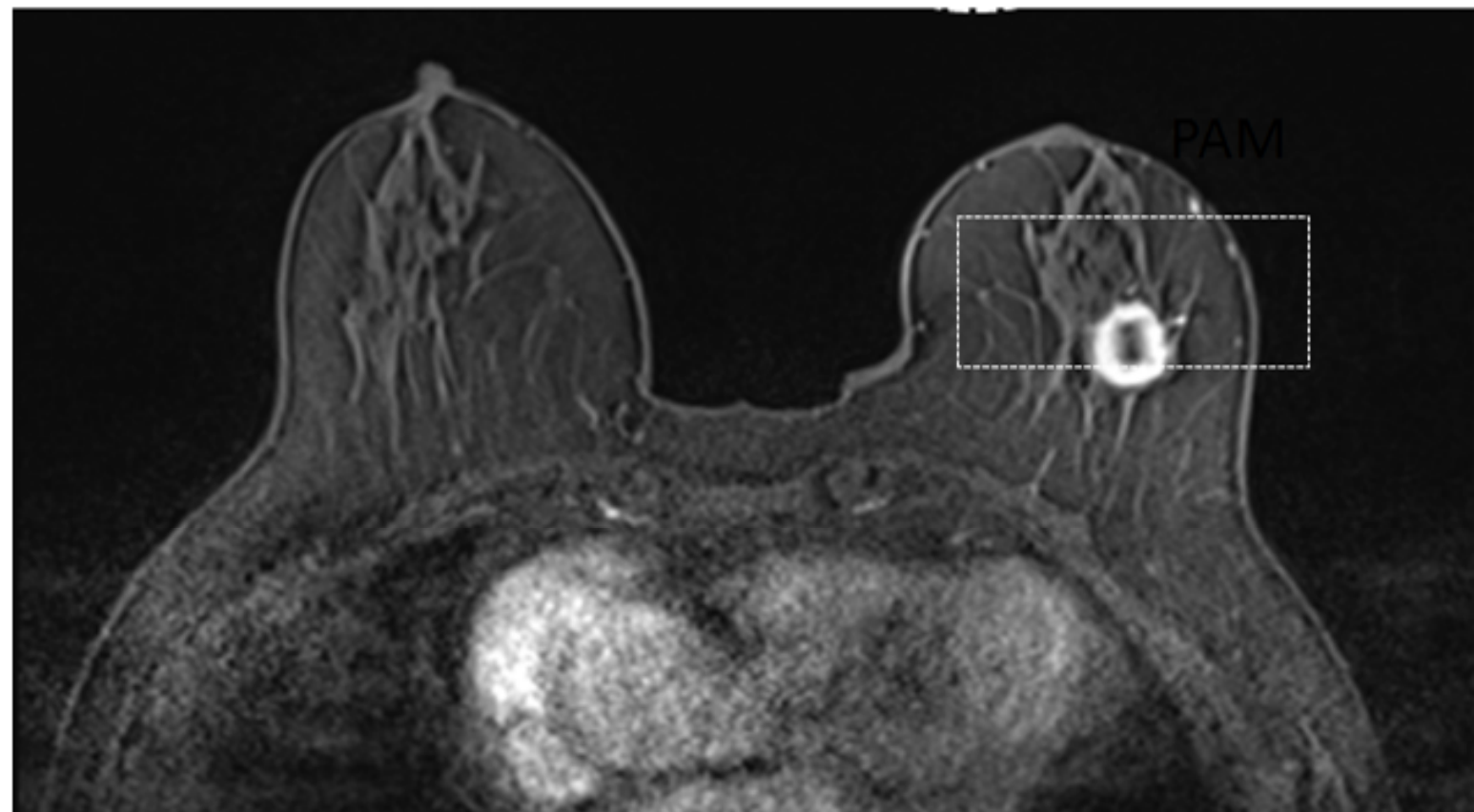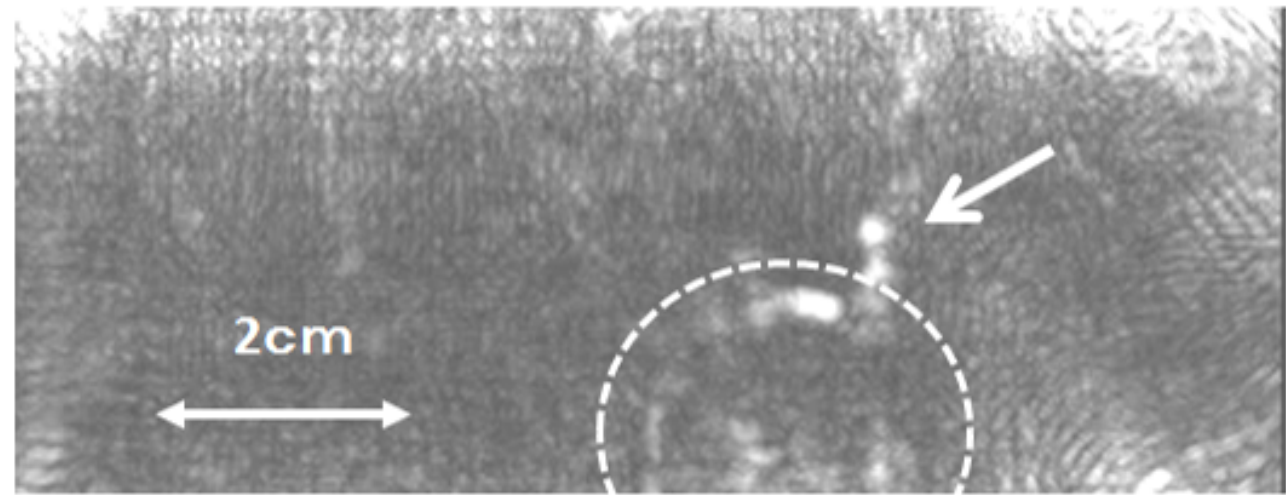
Fig. 1 a)

Fig. 1 (B)

holding plates

Patient's body

NIR laser pulse

acoustic signals

time

absorbers and thermo-elastic waves

Acoustic detector

Fig. 2

(756 nm)

Fig. 3

Fig.4
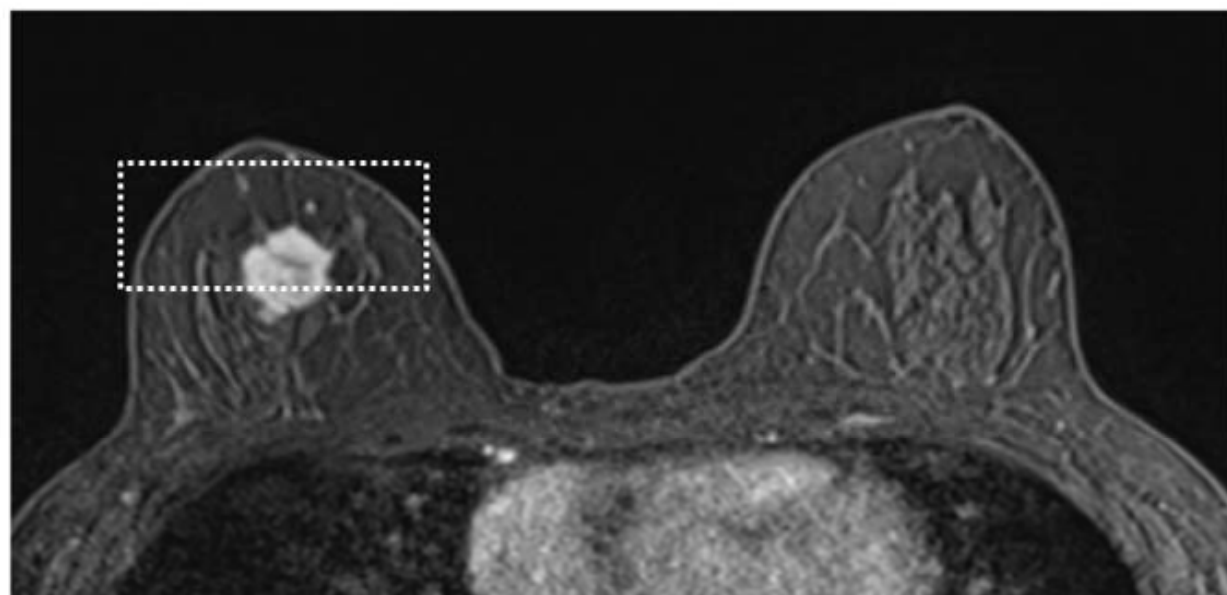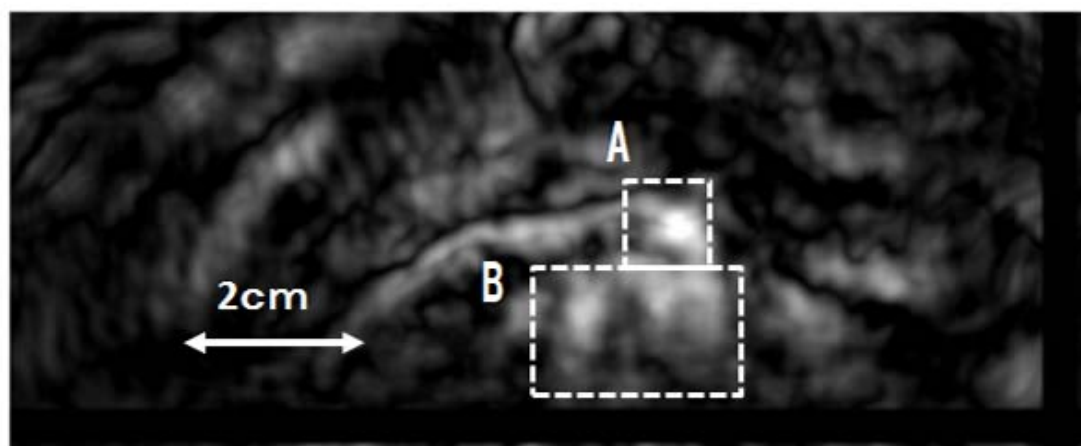
Table 1. Tumor visibility by PAM images

diagnosis	Tumor visibility
IBC without PST	8 / 12
IBC after PST	7/ 9
DCIS	5 / 5
Phyllodes tumor	0 / 1
All	20 / 27

IBC: invasive breast cancer, PST: preoperative systemic treatment, DCIS: ductal carcinoma in situ

Table 2. Results in cases of IBC without PST

Case	Diameter (MRI)	Diameter (specimen)	Pathological diagnosis	Subtype	Histological grade	PAM visibility
1	15 mm	17 mm	ILC	ER+/HER2-	2	Yes
2	28	21	IDC	ER+/HER2-	2	No
3	19	18	IDC	ER+/HER2-	2	Yes
4	13	24	IDC	ER+/HER2-	1	Yes
5	33	24	IDC	ER+/HER2-	1	No
6	15	13	IDC + DCIS	ER-/HER2+	3	Yes
7	22	18	IDC	ER+/HER2-	2	Yes
8	ND	19	IDC	ER+/HER2-	1	No
9	23	21	IDC	ER+/HER2-	2	Yes
10	22	22	IDC	ER+/HER2-	2	Yes
11	30	40	IDC	ER+/HER2-	3	No
12	19	15	IDC	ER+/HER2-	1	Yes

ND: not detectable, IDC: invasive ductal carcinoma, ILC: invasive lobular carcinoma,

DCIS: ductal carcinoma in situ, ER: estrogen receptor, HER2: her2 receptor

Table 3. Results in cases of IBC after PST

Case	Subtype	Regimen	Clinical Response	Pathological Response	Diameter	PAM visibility
1	ER+/HER2-	Let	SD	Grade 1a	10 mm	Yes
2	ER+/HER2-	Let + CPA	PR	Grade 1b~2a	8, 13	Yes
3	ER+/HER2-	Let + CPA	SD	Grade 1a	42	No
4	ER+/HER2-	Let + CPA	SD	Grade 2a	6	Yes
5	ER+/HER2-	LHRHa+Tam+5FU	SD	Grade 1b	24	Yes
6	ER-/HER2+	FEC > D + H	PR	Grade 2a	11	No
7	ER+/HER2-	TC	PR	Grade 2a	35	Yes
8	ER-/HER2-	TP > FEC	PR	Grade 2a	11	Yes
9	ER+/HER2-	AP	PR	Grade 3*	0	Yes

Let: letrozole, CPA: cyclophosphamide, FEC: epirubicine + 5-FU + cyclophosphamide, D: docetaxel,

H: herceptin, TC: docetaxel + cyclophosphamide, LHRHa: lutenizing hormone releasing hormone agonist,,

Tam: tamoxifen, TP: docetaxel + cisplatine, AP: adriamycine + cisplatine.

SD: stable disease, PR: partial response, CR: complete response.

*: DCIS remained

Table 4. Results in cases of DCIS and phyllodes tumor

Case	Diameter (MRI)	Diameter (specimen)	Pathological diagnosis	PAM visibility
1	30 mm	30 mm	DCIS, intermediate~high grade	Yes
2	11	11	DCIS, high grade	Yes
3	36	45	DCIS, intermediate grade	Yes
4	60	60	DCIS, high grade	Yes
5	70	63	DCIS, low grade	Yes
6	21	35	Phyllodes tumor, border line	No